

## Time scale for the onset of Fickian diffusion in supercooled liquids

Grzegorz Szamel and Elijah Flenner

*Department of Chemistry, Colorado State University, Fort Collins, Colorado 80525, USA*

(Received 3 August 2005; revised manuscript received 12 October 2005; published 19 January 2006)

We propose a quantitative measure of a time scale on which Fickian diffusion sets in for supercooled liquids, and we use Brownian dynamics computer simulations to determine the temperature dependence of this onset time in a Lennard-Jones binary mixture. The time for the onset of Fickian diffusion ranges between 6.5 and 31 times the  $\alpha$  relaxation time (the  $\alpha$  relaxation time is the characteristic relaxation time of the incoherent intermediate scattering function). The onset time increases faster with decreasing temperature than the  $\alpha$  relaxation time. Mean-squared displacement at the onset time increases with decreasing temperature.

DOI: [10.1103/PhysRevE.73.011504](https://doi.org/10.1103/PhysRevE.73.011504)

PACS number(s): 64.70.Pf, 61.20.Lc, 61.43.Fs

Understanding the origin of the extreme slowing down of liquids' dynamics upon approaching the glass transition and the nature of the transition itself has been of great interest for several decades. A lot of recent activity has been stimulated by the recognition that the liquids' dynamics become not only very sluggish, but also increasingly heterogeneous close to the transition [1]. While the presence of dynamic heterogeneities is commonly accepted, the details of their spatial and temporal structure have been only partially established. In particular, the question of the lifetime of dynamic heterogeneities is quite controversial. Two separate experiments [5,6] found that, near the glass transition, the lifetime is significantly longer than the  $\alpha$  relaxation time, but other experimental studies [7–9] found the lifetime to be comparable to the  $\alpha$  relaxation time. In principle, the controversy can be resolved by postulating that the temperature dependence of the lifetime is stronger than that of the  $\alpha$  relaxation time [2]. However, the physical interpretation of the new time scale remains unclear. On the computational side, there have been a few attempts to estimate the lifetime of dynamic heterogeneities. Most of them [10–13] found the lifetime to be comparable to the  $\alpha$  relaxation time. To the best of our knowledge, the only exception is a very recent paper [14] which shows that, in a kinetically constrained spin model resembling a fragile glass former, the lifetime is a few times longer than the  $\alpha$  relaxation time. More importantly, Ref. [14] found that the lifetime increases with decreasing temperature somewhat faster than the  $\alpha$  relaxation time. It should be noted that one earlier study [15] also found that, at a low temperature, the lifetime of dynamic heterogeneities is a few times longer than the  $\alpha$  relaxation time. However, a careful study of the temperature dependence of these two times has not been performed. Thus, the question of the existence of a time scale longer *and* increasing faster than the  $\alpha$  relaxation time remains unresolved.

The goal of our study is to investigate the temperature dependence of a characteristic time that is related to the lifetime of dynamic heterogeneities, the time for the onset of long-time diffusive motion. More specifically, we will study the time after which time dependence of the probability distribution of single-particle displacements can be described by Fick's law of diffusion [16]. We hereby refer to this characteristic time as the onset time for Fickian diffusion. In addition, we will investigate the temperature dependence of the

mean-squared displacement at the onset time, i.e., the distance over which the average particle has to move before it starts Fickian diffusion.

In order to define the onset time, we use an indicator of Fickian diffusion, which is the probability distribution of the logarithm of single-particle displacements,  $\log_{10}(\delta r)$ , during time  $t$ ,  $P(\log_{10}(\delta r); t)$  [17–20]. This distribution is defined in such a way that the integral  $\int_{x_0}^{x_1} P(x; t) dx$  is the fraction of particles whose value of  $\log_{10}(\delta r)$  is between  $x_0$  and  $x_1$ . The probability distribution  $P(\log_{10}(\delta r); t)$  can be obtained from the self-part of the van Hove correlation function [21],  $P(\log_{10}(\delta r); t) = \ln(10) 4\pi \delta r^3 G_s(\delta r, t)$ . The probability distribution  $P(\log_{10}(\delta r); t)$  is a convenient indicator of Fickian diffusion, because if particles move via Fickian diffusion, then the self-part of the van Hove function is Gaussian and the shape of the probability distribution  $P(\log_{10}(\delta r); t)$  is independent of time. In particular, the height of the peak of this distribution is equal to  $\ln(10) \sqrt{54/\pi} e^{-3/2} \approx 2.13$ , and deviations from this value indicate non-Fickian particle motion. We define the time for the onset of Fickian diffusion,  $\tau_F$ , as the time at which the peak of  $P(\log_{10}(\delta r); t)$  is equal to 90% of its value for a Gaussian distribution of displacements,  $P(\log_{10}(\delta r_{\max}); \tau_F) \approx 1.92$ . The threshold value of 90% may seem arbitrary at this point. We discuss this threshold value and other indicators of Fickian diffusion at the end of this paper.

It should be noted that a deviation of the probability distribution  $P(\log_{10}(\delta r); t)$  from its universal shape expected for Fickian diffusion indicates dynamic heterogeneity. However, in principle, the inverse is not necessarily true. Thus, the time for the onset of Fickian diffusion is probably only a lower bound for the lifetime of dynamic heterogeneities.

To investigate the onset time, we use the trajectories generated by an extensive Brownian dynamics simulation of a 80:20 Lennard-Jones binary mixture introduced by Kob and Andersen [22]. Briefly, the potential is given by  $V_{\alpha\beta} = 4\epsilon_{\alpha\beta}[(\sigma_{\alpha\beta}/r)^{12} - (\sigma_{\alpha\beta}/r)^6]$ , where  $\alpha, \beta \in \{A, B\}$ , and  $\epsilon_{AA} = 1.0$ ,  $\epsilon_{AB} = 1.5$ ,  $\epsilon_{BB} = 0.5$ ,  $\sigma_{AA} = 1.0$ ,  $\sigma_{AB} = 0.8$ , and  $\sigma_{BB} = 0.88$  (all the results are presented in reduced units where  $\sigma_{AA}$  and  $\epsilon_{AA}$  are the units of length and energy, respectively). A total of  $N = 1000$  particles were simulated with a fixed cubic box length of 9.4 (the details have been presented elsewhere [20,23]). In the present investigation, we use only some of

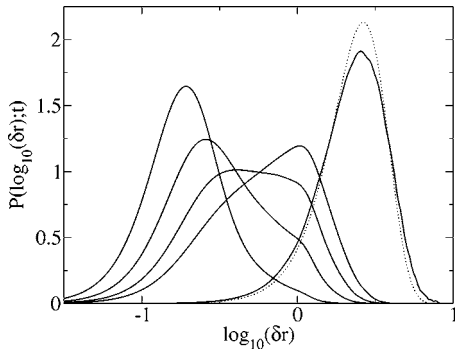


FIG. 1. The probability of the logarithm of single-particle displacements  $P(\log_{10}(\delta r); t)$  at  $T=0.45$  for the  $A$  particles. The time  $t$  is equal to, from left to right,  $\tau_{ng}=135$ ,  $\tau_{\alpha}=729$ ,  $\tau_{nng}=1550$ ,  $\tau_{0.1}=2841$ , and  $\tau_F=22391$  (see text for definition of these times). For a comparison, we also show, as a dotted line,  $P(\log_{10}(\delta r); t)$  resulting from a Gaussian distribution of displacements.

the temperatures simulated before:  $T=1.0, 0.9, 0.8, 0.6, 0.55, 0.5, 0.47$ , and  $0.45$  [24]. We present the results for the  $A$  particles only. The results for the  $B$  particles are qualitatively the same, although the statistics are worse due to the smaller number of  $B$  particles. The temperature scale is expanded by plotting various quantities versus  $T-T_c$ , where  $T_c=0.435$  is the Kob-Andersen crossover temperature [20,22]. This is a convenient way to expand the temperature scale, and it does not imply an endorsement of any particular theoretical approach.

We start by showing in Fig. 1 the probability distributions  $P(\log_{10}(\delta r); t)$  at  $T=0.45$  for the  $A$  particles at several times characteristic of the relaxation of the system. The first one is the time at which the non-Gaussian parameter  $\alpha_2(t) = \frac{3}{5} \langle \delta r^4 \rangle / \langle \delta r^2 \rangle^2 - 1$  reaches the maximum value,  $\tau_{ng}$ . The second one is the  $\alpha$  relaxation time,  $\tau_{\alpha}$ , which is defined in the usual way:  $\tau_{\alpha}$  is the time at which the incoherent intermediate scattering function for a wave vector near the peak of the static structure factor is equal to  $1/e$  of its initial time value,  $F_s(k; \tau_{\alpha})=1/e$ . The third one is the time at which a non-Gaussian parameter  $\gamma(t) = \frac{1}{3} \langle \delta r^2 \rangle \langle 1/\delta r^2 \rangle - 1$  [20] reaches its maximum value,  $\tau_{nng}$ . It should be noted that, as we argued before in Ref. [20], deviations of  $P(\log_{10}(\delta r); t)$  from its Fickian shape are most pronounced for times comparable to  $\tau_{nng}$ . The fourth one is the time at which the incoherent intermediate scattering function for a wave vector near the peak of the static structure factor is equal to 10% of its initial time value,  $F_s(k; \tau_{0.1})=0.1$ . The final one is the onset time,  $\tau_F$ , i.e., the time at which the peak of  $P(\log_{10}(\delta r); t)$  is equal to the 90% of its value for a Gaussian distribution of displacements. For comparison, we also show a  $P(\log_{10}(\delta r); t)$  resulting from a Gaussian distribution of displacements. It is clear from Fig. 1 that at shorter times, i.e., at  $\tau_{ng}$ ,  $\tau_{\alpha}$ ,  $\tau_{nng}$ , and  $\tau_{0.1}$ , the probability distributions  $P(\log_{10}(\delta r); t)$  deviate strongly from the shape resulting from a Gaussian distribution of displacements. While there are still noticeable differences even at  $\tau_F$ , we believe that these are small enough to consider  $\tau_F$  the onset time for Fickian diffusion.

In Fig. 2, we show  $P(\log_{10}(\delta r); \tau_F)$  for the  $A$  particles for  $T=1.0, 0.8, 0.6, 0.55, 0.50, 0.47$ , and  $0.45$ . It should be noted

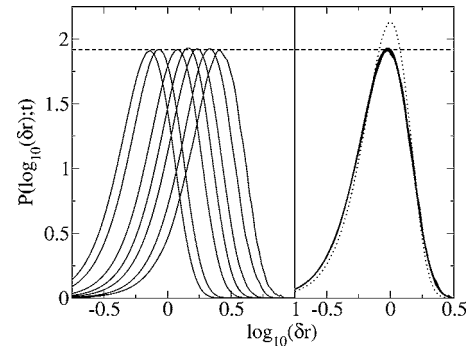


FIG. 2. Left panel: The probability of the logarithm of single-particle displacements  $P(\log_{10}(\delta r); \tau_F)$  for the  $A$  particles at  $T=1.0, 0.8, 0.6, 0.55, 0.50, 0.47$ , and  $0.45$ , listed from left to right. Right panel: the probability distributions from the left panel shifted in such a way that  $\langle \delta r^2 \rangle = 1$ ; for a comparison we also show, as a dotted line,  $P(\log_{10}(\delta r); t)$  resulting from a Gaussian distribution of displacements with  $\langle \delta r^2 \rangle = 1$ .

that with decreasing temperature the probability distributions at  $\tau_F$  shift toward larger displacements. In other words, the mean-squared displacement at the onset of Fickian diffusion increases with decreasing temperature. The right panel indicates that the shape of  $P(\log_{10}(\delta r); \tau_F)$  is temperature-independent, and, therefore, the liquid's late-time dynamics are similar up to a rescaling of the time and distance scales.

Figure 3 presents our main result: comparison of the temperature dependence of the onset time for Fickian diffusion,  $\tau_F$ , with that of the  $\alpha$  relaxation time. We find that, in the temperature range considered in this paper, the onset time is between  $6.5\tau_{\alpha}$  and  $31\tau_{\alpha}$ . More importantly, the ratio of the onset time and the  $\alpha$  relaxation time grows with decreasing temperature. Interestingly, the temperature dependence of this ratio becomes somewhat weaker with decreasing temperature, and it appears stronger in the range  $0.1 \leq T-T_c \leq 1$  than in the lower temperature range  $0.01 \leq T-T_c \leq 0.1$ .

In Fig. 4, we place the results shown in Figs. 1 and 3 in the context of the time dependence of the mean-squared displacement. On the time scale of  $\tau_{ng}$ , the mean-squared displacement has not yet reached a linear dependence on time, thus the diffusion is obviously non-Fickian. Moreover, on the

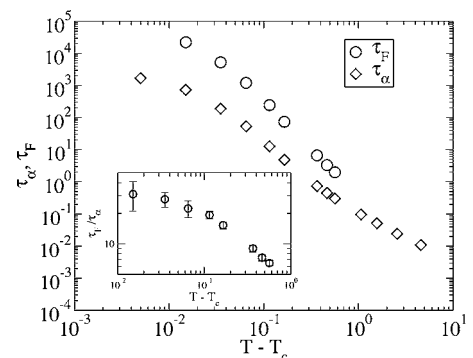


FIG. 3. Temperature dependence of characteristic times for the  $A$  particles. Diamonds: the  $\alpha$  relaxation time,  $\tau_{\alpha}$ . Circles: the onset time for Fickian diffusion,  $\tau_F$ . Inset: temperature dependence of the ratio  $\tau_F/\tau_{\alpha}$ .

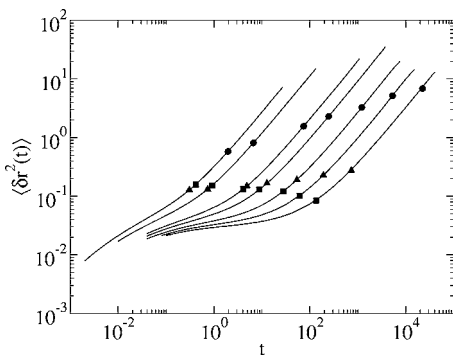


FIG. 4. The time dependence of the mean-square displacement for the A particles for  $T=1.0, 0.8, 0.6, 0.55, 0.50, 0.47,$  and  $0.45$  listed from left to right. The symbols are placed at different characteristic times. Squares: the time at which the standard non-Gaussian parameter reaches the maximum value,  $\tau_{ng}$ . Triangles: the  $\alpha$  relaxation time,  $\tau_\alpha$ . Circles: the onset time for Fickian diffusion,  $\tau_F$ .

time scale of  $\tau_\alpha$  the mean-squared displacement is, at most, at the borderline of the linear time dependence. On the other hand, the onset time,  $\tau_F$ , occurs well within the regime of apparent linear time dependence of the mean-squared displacement. Note that there is an important practical message from Fig. 4: if one monitors only the time-dependent mean-squared displacement, one can significantly underestimate the length of the run necessary to achieve Fickian diffusion.

Having identified the onset time,  $\tau_F$ , we can define a characteristic length scale, the root-mean-squared displacement at the onset time,  $[\langle \delta r^2(\tau_F) \rangle]^{1/2}$ , i.e., the distance over which the average particle has to move before it starts Fickian diffusion. It follows from Figs. 2 and 4 that this length increases with decreasing temperature and reaches 2.7 particle diameters at the lowest temperature. This is in contrast with the common belief that translational motion in moderately supercooled liquids (i.e., in liquids that can be studied in computer simulations) becomes Fickian after the particle has moved about one diameter [2].

Our characteristic length should be related to a crossover length  $l^*$  introduced by Schweizer and Saltzman via the small wave-vector expansion of the memory function [25], and by Berthier *et al.* on the basis of the analysis of kinetically constrained models [26]. The latter length was defined through the wave-vector dependence of the relaxation time of a supercooled liquid. Roughly speaking,  $l^*$  is the length scale on which diffusion is Fickian on all time scales. According to Ref. [26], this length scale changes with temperature as the square root of the product of the self-diffusion coefficient and the  $\alpha$  relaxation time,  $l^* \propto (D\tau_\alpha)^{1/2}$  [27]. In Fig. 5, we compare the temperature dependence of  $[\langle \delta r^2(\tau_F) \rangle]^{1/2}$  to that of  $l^*$ . (Note that we plot these length scales versus the  $\alpha$  relaxation time. This is in the spirit of Refs. [26,28], where it is argued that the glass transition is a manifestation of a zero-temperature critical point.) The root-mean-squared displacement at the onset time grows with increasing  $\tau_\alpha$ , and at the lowest temperatures there is an apparent scaling relationship,  $[\langle \delta r^2(\tau_F) \rangle]^{1/2} \propto \tau_\alpha^{0.13}$ . In contrast,  $(D\tau_\alpha)^{1/2}$  is initially temperature-independent. This is due to

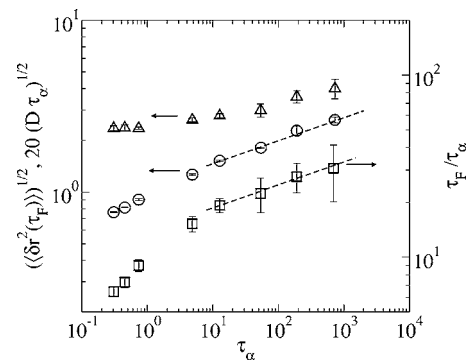


FIG. 5. Circles (left vertical axis): the root-mean-squared displacement at the onset time,  $[\langle \delta r^2(\tau_F) \rangle]^{1/2}$ . Triangles (left vertical axis): the square root of the product of the self-diffusion coefficient and the  $\alpha$  relaxation time (multiplied by 20 for convenience),  $20(D\tau_\alpha)^{1/2}$ . Squares (right vertical axis): the ratio of the onset time and the  $\alpha$  relaxation time,  $\tau_F/\tau_\alpha$ . All quantities are plotted vs the  $\alpha$  relaxation time; all the data pertain to the A particles. Dashed lines indicate the scaling relationships  $[\langle \delta r^2(\tau_F) \rangle]^{1/2} \propto \tau_\alpha^{0.13}$  and  $\tau_F/\tau_\alpha \propto \tau_\alpha^{0.13}$ .

the fact that the Stokes-Einstein relation is violated only for  $\tau_\alpha > 1$  (i.e., for  $T < 0.8$ ) [29]. However, at longer  $\alpha$  relaxation times (i.e., at lower temperatures),  $(D\tau_\alpha)^{1/2}$  has a temperature dependence similar to that of  $[\langle \delta r^2(\tau_F) \rangle]^{1/2}$ . Finally, we show in Fig. 5 that at longer  $\alpha$  relaxation times (i.e., at lower temperatures) the ratio  $\tau_F/\tau_\alpha$  appears to grow with increasing  $\alpha$  relaxation time as  $\tau_F/\tau_\alpha \propto \tau_\alpha^{0.13}$ . It is not clear whether the scaling relations indicated in Fig. 5 have any deeper significance. It could even be argued that if they continue for another seven or eight orders of magnitude of  $\tau_\alpha$  (i.e., up to  $\tau_\alpha$  comparable to that at the laboratory glass transition temperature), the resulting  $\tau_F$  would be greater than the longest experimentally observed heterogeneity lifetime.

To summarize, we proposed a quantitative definition of the onset time for Fickian diffusion and investigated its temperature dependence in a Lennard-Jones binary mixture. We found that the onset time is longer than the  $\alpha$  relaxation time and, more importantly, it increases faster with decreasing temperature than the  $\alpha$  relaxation time. Our definition of the onset time, based on the relation  $P(\log_{10}(\delta r_{\max}); \tau_F) \approx 1.92$ , seems reasonable in that it results in non-Fickian motion being present only at temperatures at and below  $T \approx 1.0$ . This temperature has been identified before as the so-called onset temperature for slow dynamics [30]. To test the robustness of our main result we tried using two other indicators of Fickian diffusion. In one approach, we used the new non-Gaussian parameter [20] and defined the onset time to be the time at which the new non-Gaussian parameter is equal to  $\frac{1}{3}$ . This particular numerical value results in non-Fickian motion being present only at temperatures at and below  $T \approx 0.8$  [31]. The resulting onset times are somewhat shorter than those shown in Fig. 3. However, the temperature dependence of the onset time defined using the new non-Gaussian parameter is similar to that of the onset time defined using  $P(\log_{10}(\delta r); t)$ . In addition, we found that the shapes of  $P(\log_{10}(\delta r); t)$  at the onset times defined using the new non-Gaussian parameter are very similar. In particular, the height

of the peak is approximately temperature-independent and equal to 85% of its value for Fickian diffusion. In an alternative approach, we used the standard non-Gaussian parameter  $\alpha_2(t)$  and defined the onset time using the threshold value of 0.2. The resulting onset times are close to those obtained from the new non-Gaussian parameter with a slightly higher threshold value of  $\frac{1}{3}$ . When the threshold value used for the standard non-Gaussian parameter is lowered to 0.135, the onset times obtained approximately agree with those obtained from the probability distribution  $P(\log_{10}(\delta r); t)$ .

The results presented here call for a further simulational investigation of dynamic heterogeneities on time scales longer than the  $\alpha$  relaxation time [32]. Also, it would be interesting to use probability distributions of single-particle displacements obtained in confocal microscopy investiga-

tions of colloidal dynamics [33] to investigate the volume fraction dependence of the Fickian diffusion onset time in real colloidal systems.

Finally, we would like to point out that the results presented here violate the time-temperature superposition principle. In order to superimpose the probability distributions  $P(\log_{10}(\delta r); t)$  shown in the left panel of Fig. 2, we have to shift  $\log_{10}(\delta r)$  by  $\log_{10}[\langle \delta r^2(\tau_F) \rangle]^{1/2}$ . The typical shift procedure, agreeing with the time-temperature superposition principle, would involve the  $\alpha$  relaxation time rather than the onset time  $\tau_F$ , which has a temperature dependence different from  $\tau_\alpha$ .

G.S. thanks Mark Ediger for many discussions that stimulated this work. We gratefully acknowledge the support of NSF Grants No. CHE 0111152 and CHE 0517709.

- 
- [1] Experimental studies of dynamic heterogeneities have been reviewed in Refs. [2,3]. For a very recent review of simulational investigations, see Ref. [4].
- [2] M. D. Ediger, *Annu. Rev. Phys. Chem.* **51**, 99 (2000).
- [3] R. Richert, *J. Phys.: Condens. Matter* **14**, R703 (2002).
- [4] H. C. Andersen, *Proc. Natl. Acad. Sci. U.S.A.* **102**, 6686 (2005).
- [5] M. T. Cicerone and M. D. Ediger, *J. Chem. Phys.* **103**, 5684 (1995); C.-Y. Wang and M. D. Ediger, *J. Phys. Chem. B* **103**, 4177 (1999).
- [6] L. A. Deschenes and D. A. Vanden Bout, *Science* **292**, 255 (2001).
- [7] R. Böhmer *et al.*, *Europhys. Lett.* **36**, 55 (1996); R. Böhmer, G. Diezemann, G. Hinze, and H. Sillescu, *J. Chem. Phys.* **108**, 890 (1998).
- [8] M. Yang and R. Richert, *J. Chem. Phys.* **115**, 2676 (2001).
- [9] B. Schiener, R. Böhmer, A. Loidl, and R. V. Chamberlin, *Science* **274**, 752 (1996).
- [10] D. N. Perera and P. Harrowell, *J. Chem. Phys.* **111**, 5441 (1999).
- [11] B. Doliwa and A. Heuer, *J. Non-Cryst. Solids* **307–310**, 32 (2002).
- [12] E. Flenner and G. Szamel, *Phys. Rev. E* **70**, 052501 (2004).
- [13] Y. Jung, J. P. Garrahan, and D. Chandler, *J. Chem. Phys.* **123**, 084509 (2005).
- [14] S. Leonard and L. Berthier, *J. Phys.: Condens. Matter* **17**, S3571 (2005).
- [15] R. Yamamoto and A. Onuki, *Phys. Rev. Lett.* **81**, 4915 (1998).
- [16] D. Chandler, *Introduction to Modern Statistical Mechanics* (Oxford, New York, 1987).
- [17] A. M. Puertas, M. Fuchs, and M. E. Cates, *J. Chem. Phys.* **121**, 2813 (2004).
- [18] M. E. Cates *et al.*, *J. Phys.: Condens. Matter* **16**, S4861 (2004).
- [19] D. R. Reichman, E. Rabani, and P. L. Geissler, *J. Phys. Chem. B* **109**, 14654 (2005).
- [20] E. Flenner and G. Szamel, *Phys. Rev. E* **72**, 011205 (2005).
- [21] J. P. Hansen and J. R. McDonald, *Theory of Simple Liquids*, 2nd ed. (Academic, London, 1986).
- [22] W. Kob and H. C. Andersen, *Phys. Rev. Lett.* **73**, 1376 (1994); *Phys. Rev. E* **51**, 4626 (1995); **52**, 4134 (1995).
- [23] G. Szamel and E. Flenner, *Europhys. Lett.* **67**, 779 (2004).
- [24] The previous runs at the temperature  $T=0.45$  have been extended by 100%; the  $A$  particles' mean-squared displacement at the end of the extended runs is about 19.
- [25] K. S. Schweizer and E. J. Saltzman, *J. Phys. Chem. B* **108**, 19729 (2004).
- [26] L. Berthier, D. Chandler, and J. P. Garrahan, *Europhys. Lett.* **69**, 320 (2005).
- [27] B. M. Erwin, R. H. Colby, S. Y. Kamath, and S. K. Kumar (e-print cond-mat/0409778), on the basis of dimensional analysis, proposed the same formula for a different length scale, the so-called cooperative length scale.
- [28] J. P. Garrahan, and D. Chandler, *Phys. Rev. Lett.* **89**, 035704 (2002); S. Whitlam, L. Berthier, and J. P. Garrahan, *ibid.* **92**, 185705 (2004).
- [29] E. Flenner and G. Szamel, *Phys. Rev. E* **72**, 031508 (2005).
- [30] Y. Brumer and D. R. Reichman, *Phys. Rev. E* **69**, 041202 (2004).
- [31] Note that, according to both definitions, the appearance of the non-Fickian motion correlates with the violation of the Stokes-Einstein relation.
- [32] So far simulational studies mostly investigated heterogeneities on the  $\tau_{ng}$  time scale; for a study of longer-time-scale heterogeneities, see N. Lačević *et al.*, *J. Chem. Phys.* **119**, 7372 (2003).
- [33] W. K. Kegel and A. van Blaaderen, *Science* **287**, 290 (2000); E. R. Weeks *et al.*, *ibid.* **287**, 627 (2000).